Journal of Water Sciences & Environment Technologies

Cite this: *JOWSET, **2019** (04), N°01, 472-479*

Adsorption of Methylene Blue Dye by Activated Carbon Prepared from Malted Sorghum Mash and Plantain Peels

Emmanuel Olajide Oyelude*, Eugene Osei Akoto, Raymond Penyindiey

Department of Applied Chemistry and Biochemistry, University for Development Studies, Navrongo Campus, P.O. Box 24, Navrongo, NV, Ghana

**Corresponding Author: Tel.: +233 (0)24 668 1133; e-mail: emmanola@gmail.com*

The feasibility of using an activated carbon prepared from teak leaf litter and cocoa pod husks (MPAC) to remove methylene blue (MB) from aqueous solution was investigated. The effects of contact time, MPAC dosage, initial concentration, pH and temperature of MB solution were investigated through adsorption equilibrium, isotherm, kinetic and thermodynamic studies. Optimum adsorption of MB from solution occurred at pH 8 and low adsorbent dosages. The physical adsorption process was endothermic and best described by Langmuir isotherm, pseudo-second order kinetic models and liquid film diffusion mechanism. MPAC is a promising adsorbent for removing MB from aqueous solution.

Received: 16 January 2019
Accepted: 13 June 2019
Available online: 24 June 2019

Keywords:
Adsorption,
Activated Carbon,
Methylene Blue,
Isotherm,
Kinetics,
Thermodynamics,

Introduction

Many industries worldwide produce dye-contaminated wastewaters which may pose danger to the environment if not properly treated before disposal or reuse. An estimated 14,000 ton of dyes is released into the environment annually [1]. The negative impacts associated with the presence of color in water have been documented [2, 3].

A number of techniques are available for removing dyes from wastewaters with different merits and demerits bothering on efficiency, cost, speed of operation, level of complexity, ease of handling by-products and safety [3-5]. Adsorption is a popular technique for treating dye-polluted wastewaters due to its simplicity, convenience and ease of operation [6]. Commercial activated carbon is the most sought after adsorbent for removing pollutants from aqueous solution. However, poor selectivity properties and prohibitive procurement and regeneration costs are noteworthy drawbacks to its acceptance [7].

Plant-based materials have been touted as viable resources for producing effective low-cost adsorbents because they are cheap, abundant, renewable, biodegradable and environmentally friendly [8]. A striking characteristic of low-cost adsorbents is their low surface area which rarely surpasses 50 m^2/g [9] without modification. The conversion of plant-based materials to activated carbon tends to improve their surface areas tremendously. The reported surface area of selected laboratory-prepared low-cost activated carbons are: 741, 774, 783, 943 and 1114 m^2/g for *Euphorbia rigida* biomass, walnut shell, almond shell, corn cob and groundnut shell [10-14], respectively.

In the present study, low-cost activated carbon was prepared from malted sorghum mash and plantain peels. The equilibrium adsorption, kinetic and thermodynamics of the adsorbent to remove methylene blue (MB) dye from aqueous solution were investigated.

Materials and methods

1. Materials

1.1. Preparation of Activated Carbon

Malted sorghum mash (MSM), a by-product of local sorghum-based beverage called *pito*; was sourced from a brewer at Navrongo, north-eastern Ghana. The material was pretreated as earlier described [15]. Plantain peels (PP) were collected from food vendors operating around the university campus at Navrongo. They were stripped of foreign matter and dried under the sun for two weeks. Potassium salt was extracted from PP according to the method developed at Cocoa Research Institute of Ghana [16].

MSM was carbonized in a furnace (Thermolyne F48010-33) at 400°C for 1 h and allowed to cool. Some distilled water was added to 1:1 (w/w) mixture of carbonized MSM and the potassium salt and thoroughly mixed. The mixed precursors were dried overnight at 105°C in an oven (Binder 9110-0305) and later activated in a furnace at 500°C for 1 h. The activated carbon produced was cooled and washed several times with 2% (v/v) HCl and distilled water the wash water had pH 7 ± 0.2. The produced activated carbon was dried overnight at 105°C and cooled in a desiccator. The final product was ground, sieved to particle size below 210 µm and stored in a corked glass bottle labeled “MPAC”.

1.2. Methylene Blue

The methylene blue (MB) dye used was produced by Merck (Darmstadt, Germany) and used as received. A 1000-mg/L stock solution was prepared from which dilute working solutions were prepared as needed.

2. Experimental Methods

2.1 Characterization of MPAC

The Fourier transform infrared (FTIR) absorption spectrum was recorded using Perkin Elmer spectrophotometer [7]. Moisture, volatile matter, ash and fixed carbon were all determined as described by Jeyakumar and Chandrasekaran [18]. Calibrated pH meter was used to determine the pH [19] and bulk density was determined using 50 mL measuring cylinder [20]. The specific surface area was estimated by the method proposed by Sears Jr. [21].

2.2 Equilibrium Adsorption Studies

Equilibrium adsorption experiments were conducted at room temperature except where indicated otherwise [22]. The concentration of the residual dye was determined at λ_{max} of 668 nm using uv/visible spectrophotometer (Jenway 6305). The quantity of MB adsorbed by MPAC, q_e (mg/g) or R (%) was calculated thus:

$$q_e = \frac{(C_o - C_e)V}{w} \quad (1)$$

and

$$R = \frac{(C_o - C_e)}{C_o} \times 100 \quad (2)$$

where C_o (mg/L) and C_e (mg/L) are the initial and equilibrium concentration of MB, respectively; V (L) is the volume of MB solution and w (g) is the mass of MPAC. Each experiment was conducted three times and the average value recorded. Every determination that differed by more than 5% from the average value was excluded and repeated.

Adsorption experiments were conducted in 250 mL Erlenmeyer flasks containing 100 mL of dye solution and predetermined mass of MPAC. The flasks were agitated at 100 rpm until equilibrium was attained. The effects of contact time and the initial concentration of MB were assessed at room temperature by varying the concentration of the dye from 25 to 200 mg/L. All experiments attained equilibrium on or before 80 min. Therefore, the contact time for subsequent experiments was fixed at 100 min except for the study of adsorption kinetics. The impact of MPAC dosage was studied by varying the mass of MPAC from 0.05 g to 1 g.

The impact of pH of dye solution was investigated by adjusting the pH of MB from 2 to 10 using 0.1 M HCl and 0.1 M NaOH solutions. The influence of temperature on uptake of MB by MPAC was studied at temperature between 303 and 318 K.

2.3 Adsorption Isotherm

The data for adsorption isotherm were generated by fixing the mass of MPAC and the volume, pH and temperature of MB solution at 0.05 g, 100 mL, pH 8 and 298 ± 1°C, respectively. The concentration of MB solution was varied at 20 mg/L interval from 20 to 140 mg/L.

2.4 Adsorption Kinetics

Adsorption kinetics experiments were conducted by varying the concentration of MB between 25 and 200 mg/L. However, the mass of MPAC was set at 0.05 g while the volume, pH and temperature of the dye solution were fixed at 100 mL, pH 8 and 298 ± 0.5°C, respectively.

2.5 Adsorption Thermodynamics

The values of enthalpy (ΔH, kJ/mol), entropy (ΔS, J/mol K), and free energy (ΔG, kJ/mol) were determined by conducting adsorption experiments from 303 to 318 K, similar to that of the effect of temperature on uptake of MB by MPAC.

Results and discussion

1. Characteristics of MPAC

The average yield of the MPAC produced was 39.61%. The average moisture content, bulk density and pH of the adsorbent were: 9.14%, 0.45 g/cm^3 and 7.12, respectively. The adsorbent is slightly basic in nature. The bulk density of MPAC is comparable to 0.47 g/cm^3 reported for a commercial activated carbon [22].

The average values of moisture content, volatile matter, ash and fixed carbon of MPAC were: 9.14%, 8.26%, 2.61% and 79.99%, respectively. The mean surface area of MPAC was 289.80 m^2/g. This value is lower than 324.79 m^2/g reported for activated carbon produced from pongam seed shell [23] but higher than 234 m^2/g obtained for activated carbon from green teak leaves [24].

2. Effects of Contact Time and Initial Concentration of MB

The rate of removal of MB from aqueous solution by MPAC was swift at the early stages with uptake of at least 75% of the total dye adsorbed occurring within the first 20 min as shown in Fig. 1. The fast uptake of the dye at the early stages is due to the existence of large number of binding sites on the adsorbent [25]. The contact time required for the system to attain equilibrium is influenced by the initial concentration of the MB solution. For instance, 25 and 200 mg/L dye solution required 40 and 80 min contact time, respectively to attain equilibrium. On the basis of these results, the contact time for subsequent experiments was fixed at 100 min.

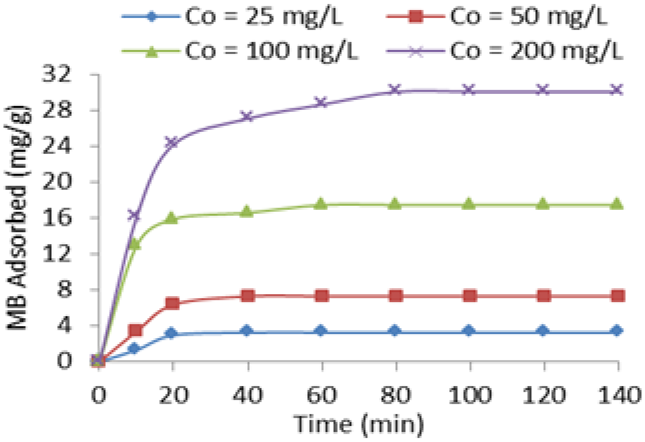

Fig. 1: Effects of contact time and initial concentration of dye on adsorptive removal of MB by MPAC, (V: 100 mL, w: 0.5 g)

The quantity of dye adsorbed by MPAC from solution at equilibrium improved from 3.25 to 30.12 mg/g as the initial concentration of MB was raised from 25 to 200 mg/L. This observation is attributed to reduction in resistance to adsorption of dye because of the driving force provided by concentration gradient [26].

3. Effect of MPAC Dosage

The change in dosage of the adsorbent exerted a noteworthy influence on dye uptake as presented in Fig. 2. The quantity of MB removed increased from 64.7 to 74.6% when the MPAC dosage was increased from 0.5 to 10 g/L. The boost in the uptake of MB by MPAC was due to the availability of extra binding sites as the mass of the adsorbent increased. The actual adsorption density, however, plummeted from 64.7 to 3.7 mg/g for the same change in adsorbent dosage. The inverse relationship between dosage and adsorption capacity is attributed to a combination of fast superficial uptake of dye molecules at higher dosages and aggregation of adsorbent particles [27, 28].

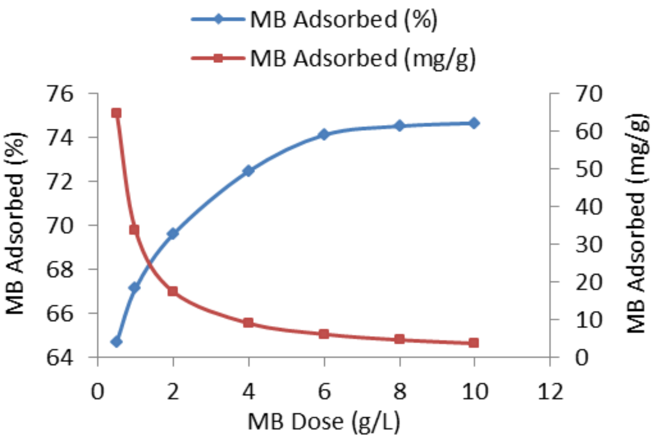

Fig. 2: Effect of adsorbent dosage on adsorptive removal of MB by MPAC, (C_0: 50 mg/L, V: 100 mL, w: 0.05 – 1 g)

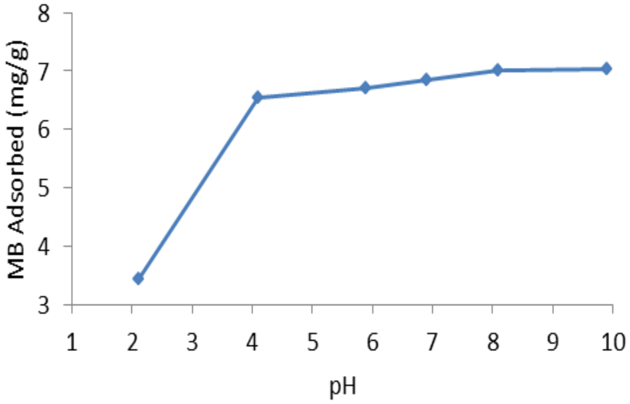

Fig. 3: Effect of pH of dye solution on adsorptive removal of MB by MPAC, (C_0: 50 mg/L, V: 100 mL, w: 0.5 g)

4. Effect of pH of MB Solution

The influence of pH on removal of ionic adsorbates from aqueous solution is often weighty. The result of the impact of initial pH of MB solution on its removal by MPAC is presented in Fig. 3. Uptake of MB from aqueous solution rose sharply from 3.4 mg/g at pH 2 to 6.6 mg/g at pH 4 and gradually increased to 7.0 mg/g at pH 8 where it stabilized. The poor adsorption of the dye below pH 4 is ascribed to competition between protons (H^+) and cationic MB for binding sites on the surface of MPAC [29].

The surface of the adsorbent became negatively charged when pH was increased beyond that of the point of zero charge of the adsorbent. Hence, removal of the MB was boosted through electrostatic attraction between the cationic dye and the negatively charged surface of MPAC [30]. Similar result was obtained by Bestani and his team members who used activated leaves of *Salsola vermiculata* to adsorb MB from aqueous solution [31].

5. **Effect of Temperature of MB Solution**

The adsorption of MB from aqueous solution was influenced by temperature as shown in Fig. 4. The quantity of dye removed by the adsorbent improved from 25.6 to 29.0 mg/g when the temperature was raised from 303 to 318 K. The adsorptive removal of MB from aqueous solution by MPAC was therefore an endothermic process [28, 32].

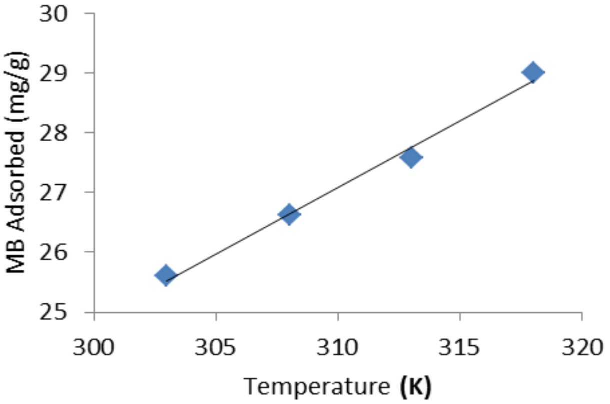

Fig. 4: Effect of temperature on adsorptive removal of MB by MPAC, (C_o: 50 mg/L, V: 100 mL, w: 0.05 g)

6. **Adsorption Isotherm**

Adsorption isotherm is essential to better understand the interaction between an adsorbent and an adsorbate [33] and for designing effective adsorption systems [31]. The Langmuir [34], Freundlich [35] and Dubinin-Radushkevich [36] isotherm models were used to assess the equilibrium adsorption of MB onto MPAC.

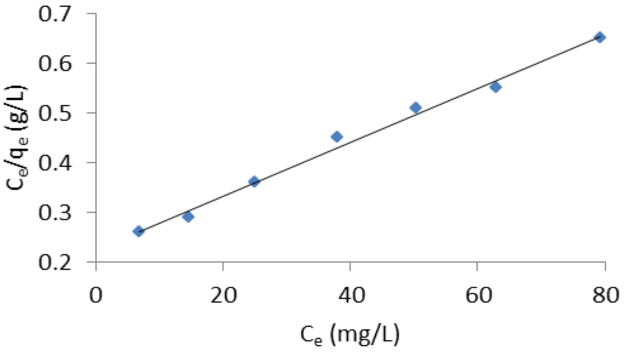

Fig. 5: Langmuir isotherm plot for adsorption of MB onto MPAC (C_o = 20 – 140 mg/L, V = 100 mL, w = 0.05 g, pH 8, T = 298 K)

Langmuir model [34] assumes monolayer adsorption, homogenous adsorbent surface and, hence, constant energy of adsorption on the surface of the adsorbent [37]. The linear form of Langmuir equation is

$$\frac{C_e}{q_e} = \frac{1}{q_m} C_e + \frac{1}{q_m}\frac{1}{K_L} \tag{3}$$

Where C_e (mg/L) is the equilibrium concentration of MB, q_e (mg/g) is the mass of MB adsorbed at equilibrium per gram of MPAC, q_m (mg/g) is the monolayer adsorption capacity of MPAC and K_L (L/mg) is the Langmuir constant. The values of q_m and K_L are determined from the slope and intercept of the plot of C_e/q_e versus C_e presented in Fig. 5. A dimensionless separation factor, R_L, defined as

$$R_L = \frac{1}{(1 + K_L C_o)} \tag{4}$$

was used to assess the applicability of the Langmuir equation; where C_o (mg/L) represents the highest initial concentration of MB. Adsorption is termed favorable if $0 < R_L < 1$ [38].

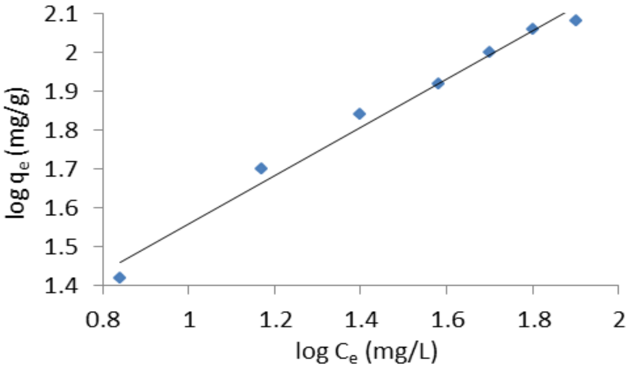

Fig. 6: Freundlich isotherm plot for adsorption of MB onto MPAC (C_o = 20 – 140 mg/L, V = 100 mL, w = 0.05 g, pH 8, T = 298 K)

Freundlich isotherm is applicable to an adsorbent with heterogeneous surface and multilayer or continuous adsorption [35]. Its linear form is

$$\log q_e = \frac{1}{n} \log C_e + \log K_F \tag{5}$$

where K_F ($mg^{1-1/n}L^{1/n}/g$) and 1/n represent the Langmuir constant and the heterogeneity factor, respectively. The values of K_F and 1/n are obtained from the plot of log q_e against log C_e shown in Fig. 6.

Dubinin-Radushkevich isotherm [36] is applied to assess the mean adsorption free energy and the nature of adsorption. Its linear equation is

$$\ln q_e = \ln q_{DR} - \beta \varepsilon^2 \qquad (6)$$

where q_{DR} (mol/g) represents the Dubinin-Radushkevich monolayer adsorption capacity, β (mol^2/J^2) is activity coefficient and Ɛ represents the Polanyi potential given by

$$\varepsilon = RT \ln\left(1 + \frac{1}{C_e}\right) \qquad (7)$$

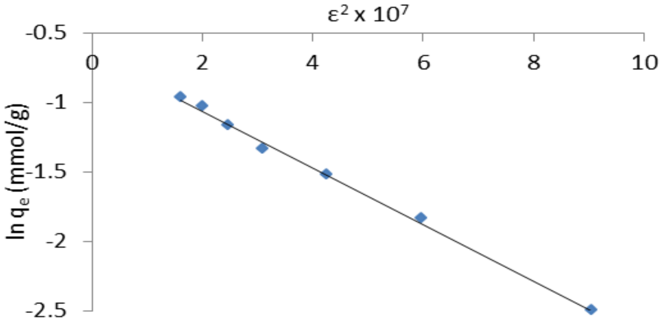

Fig. 7: Dubinin-Radushkevich isotherm plot for adsorption of MB by MPAC (C_o = 20 – 140 mg/L, V = 100 mL, w = 0.05 g, pH 8, T = 298 K)

R (8.314 J/mol K) and T (K) are the gas constant and temperature, respectively. The values of q_{DR} and β (Tab. 1) are obtained from the linear plot of ln q_e versus $Ɛ^2$ presented in Fig. 7. The mean energy, E (J/mol), is estimated from the relationship

$$E = \frac{1}{\sqrt{2\beta}} \qquad (8)$$

Generally, adsorption is said to be physical in nature if 0 < E < 8 kJ/mol and chemical in nature if 8 < E < 16 kJ/mol [39].

Tab. 1: Isotherm constants for adsorption of MB by MPAC

Parameter	Isotherm		
	Langmuir	Freundlich	D-R
K_L (L/mg)	7.7084		
q_m (mg/g)	185.18		
R_L	0.2286		
K_F ($mg^{1-1/n}L^{1/n}/g$)		8.7217	
1/n		0.6194	
q_{DR} (mmol/g)			0.5175
q_{DR} (mg/g)			165.53
E (kJ/mol)			5.0000
R^2	0.9918	0.9838	0.9968

Note: D-R = Dubinin-Radushkevich

The high correlation coefficient (R^2 = 0.9918) for Langmuir model and the fact that the value of 1/n (Freundlich model) is lesser than unity confirm that the process is a normal Langmuir isotherm [40]. The surface of MPAC is, therefore, fairly homogenous and the adsorption of MB onto it is favorable (R_L = 0.2286). The maximum monolayer adsorption capacity of MPAC is 185.18 mg/g. The adsorption process is physical in nature because the calculated mean free energy is 5.00 kJ/mol. The values of all relevant isotherm parameters, constants and correlation coefficients (R^2) are displayed in Table 1.

7. **Adsorption Kinetics**

The kinetics of adsorption provides insight into how far the process progresses towards equilibrium as well as the mechanism governing the removal of the adsorbate by the adsorbent [41]. Adsorption kinetics data were analyzed using pseudo-first order [42], pseudo-second order [43], intraparticle diffusion [44] and liquid film diffusion [45] models.

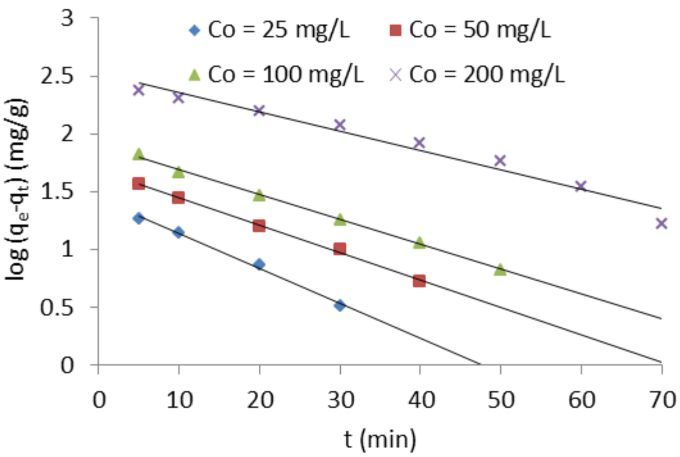

Fig. 8: Pseudo-first order kinetic plot for adsorption of MB onto MPAC (V = 100 mL, w = 0.05 g, pH 8, T = 298 K)

The linearized pseudo-first order, pseudo-second order, intraparticle diffusion and liquid film diffusion equations are presented in equations 9, 10, 11 and 12, respectively

$$\ln(q_e - q_t) = \ln q_e - k_1 t \qquad (9)$$

$$\frac{t}{q_t} = \frac{1}{k_2 q_e^2} + \frac{1}{q_e} t \qquad (10)$$

$$q_t = k_{id} t^{1/2} + C \qquad (11)$$

$$\ln\left(-\frac{q_t}{q_e}\right) = -k_{fd} t \qquad (12)$$

where q_t (mg/g) and q_e (mg/g) are the quantity of adsorbate removed per gram of adsorbent at time, t (min) and at equilibrium, respectively. Moreover, C is a constant related to the boundary layer; k_1 (1/min), k_2 (g/mg.min), k_{id} (mg/g.min$^{1/2}$) and k_{fd} (1/min) are the pseudo-first order, pseudo-second order, intraparticle diffusion and liquid film diffusion rate constants, respectively. The initial rate of adsorption, h (mg/g.min), is calculated from the pseudo-second order model using equation 13.

$$h = k_2 q_e^2 \tag{13}$$

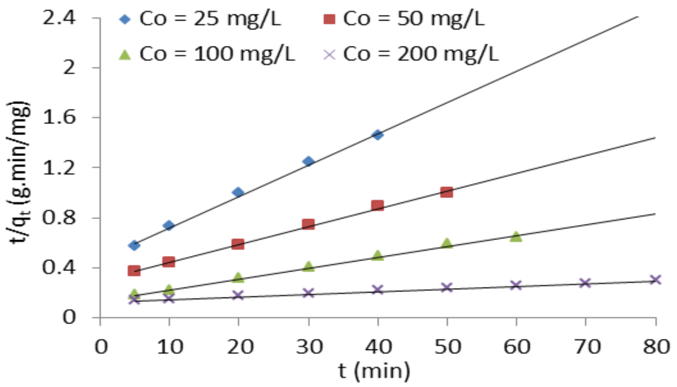

Fig. 9: Pseudo-second order kinetic plot for adsorption of MB onto MPAC (V = 100 mL, w = 0.05 g, pH 8, T = 298 K)

The linear plots for the four adsorption kinetic models employed are presented in Figs 8, 9, 10 and 11. The values of relevant parameters, constants and correlation coefficients (R^2) are displayed in Table 2. The process is best described by the pseudo-second order model on the basis of the R^2 values at all initial concentrations and closeness of the experimental and calculated values of q_e.

The intraparticle and liquid film diffusion models were employed to decipher the rate controlling step. On the average, the plots for the latter (Fig. 11) fit better and all the plots pass through the origin. This confirms the liquid film diffusion as the rate-determining step in the adsorption process [47].

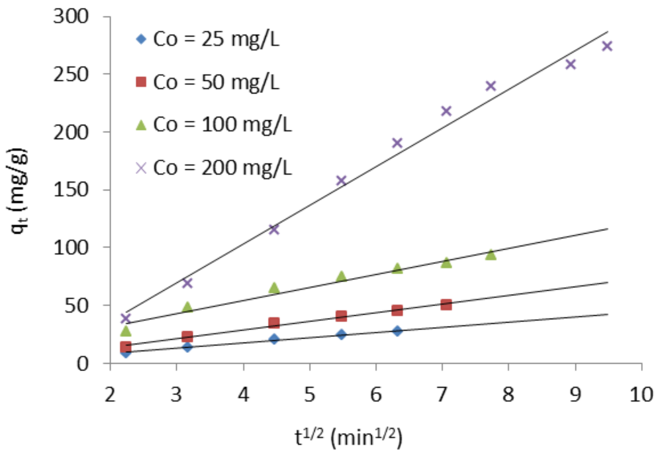

Fig. 10: Intraparticle diffusion kinetic plot for adsorption of MB onto MPAC (V = 100 mL, w = 0.05 g, pH 8, T = 298 K)

8. **Adsorption Thermodynamics**

The equation relating the change in Gibbs free energy (ΔG), enthalpy (ΔH) and entropy (ΔS) is

$$\Delta G = \Delta H - T\Delta S \tag{14}$$

The values of ΔG, at different temperatures were calculated by applying.

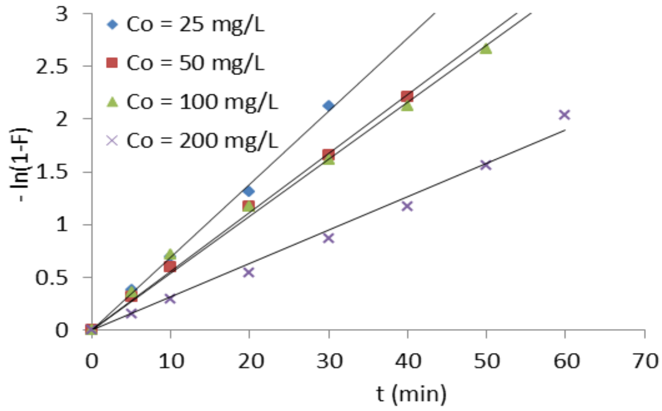

Fig. 11: Liquid film diffusion kinetic plot for adsorption of MB onto MPAC (V = 100 mL, w = 0.05 g, pH 8, T = 298 K)

Tab. 2: Kinetic constants for adsorption of MB onto MPAC

Kinetic Models	**C_0 (mg/L)**			
	25	**50**	**100**	**200**
Pseudo-First Order				
$q_{e,cal}$ (mg/g)	4.2135	5.3919	6.6926	12.407
$q_{e,exp}$ (mg/g)	27.500	50.240	93.120	274.44
k_1 (g/mg min)	0.0302	0.0238	0.0215	0.0167
R^2	0.9938	0.9975	0.9973	0.9669
Pseudo-Second Order				
$q_{e,cal}$ (mg/g)	39.841	69.930	114.94	276.19
$q_{e,exp}$ (mg/g)	27.500	50.240	93.120	274.44
k_2, (g/mg.min)	0.0013	0.0007	0.0006	0.0001
h (mg/g.min)	2.1313	3.3367	7.4239	8.1301
R^2	0.9963	0.9977	0.9969	0.9969
Intraparticle Diffusion				
k_{id} (mg/g.min$^{1/2}$)	4.5980	7.4856	11.267	33.555
C (mg/g)	1.0717	1.4694	9.3262	31.428
R^2	0.9961	0.9862	0.9658	0.9869
Liquid Film Diffusion				
k_{fd} (1/min)	0.0692	0.0559	0.0540	0.0315
R^2	0.9969	0.9982	0.9912	0.9876

$$\Delta G^{o} = -RT \ln K_{d} \quad (15)$$

and

$$K_{d} = \frac{C_{s}}{C_{e}} \quad (16)$$

where K_d is the distribution coefficient, C_s (mg/L) is the quantity of dye adsorbed by MPAC at equilibrium and C_e (mg/L) is the quantity of dye in solution at equilibrium.

The equalization of equations 14 and 15 to eliminate ΔG produces

$$\ln K_{d} = \frac{\Delta S}{R} - \frac{\Delta H}{RT} \quad (17)$$

The Van't Hoff plot of ln K_d versus 1/T (Fig. 12) facilitated the determination of the values of ΔH and ΔS. The calculated values of ΔG, ΔH and ΔS from 303 to 318 K are presented in Table 3. The negative values of ΔG established the feasibility of the process. The positive value ΔH confirmed that the adsorption was an endothermic process. The positive value of ΔS indicates increased disorder at the MPAC-MB solution interface during the adsorption process [46].

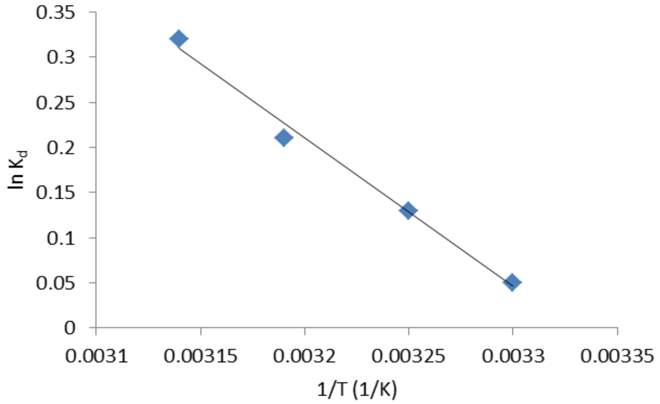

Fig. 12: Van't Hoff plot for adsorption of MB onto MPAC (C_o = 50 mg/L, V = 100 mL, w = 0.05 g, pH 8, T = 298 K)

Tab. 3: Thermodynamic parameters for adsorption of MB onto MPAC

ΔG (kJ/mol)				ΔH (kJ/mol)	ΔS (J/mol.K)
303 K	308 K	313 K	318 K		
-0.13	-0.33	-0.55	-0.85	13.67	45.48

Conclusions

In this study, a low-cost MPAC activated carbon was produced from teak leaf litter and potassium salt extracted from plantain peels. The adsorbent was successfully used to remove MB from aqueous solution. The adsorption process was feasible and influenced by contact time, initial concentration of dye solution, MPAC dosage, pH of MB solution and temperature. Optimum adsorption of dye per gram of adsorbent occurred at pH 8 and low adsorbent dosages. The estimated Langmuir monolayer capacity of the adsorbent was 185.18 mg/g. Pseudo-second order model best fit the kinetic data. The free energy (5.00 kJ/mol) estimated from Dubinin-Radushkevich isotherm established the process as physical adsorption. The removal of the dye by the adsorbent was spontaneous and endothermic in nature. In conclusion, the capacity of the adsorbent, isotherm, kinetic and thermodynamic studies conducted indicated that MPAC is a promising low-cost adsorbent for removal of MB from aqueous solution.

References

1. J.A. González, M.E. Villanueva, L.L. Piehl, G.J. Copello. *Chem. Eng. J.* **2015**, 280, 41
2. S-T. Ong, P-S. Keng, W-N. Lee, S-T. Ha, Y-T. Hung. *Water* **2011**, 3, 157
3. M. Ejder-Korucu, A. Gürses, Ç. Doğăr, S.K. Sharma, M. Açikyildiz. Removal of organic dyes from industrial effluents: An overview of physical and biotechnological applications in: *Green chemistry for dyes removal in wastewaters* (S.K. Sharma, ed.), Scrivener Publishing, **2015**.
4. A. Gürses, M. Açikyildiz, K. Güneş, M.Z. Gürses. *Dyes and pigments: Springer briefs in green chemistry for sustainability*, Springer, Switzerland, **2016**.
5. A. Ashfaq, A. Khatoon. *Intl J. Current Microbiol. Appl. Sci.* **2014**, 3(7), 780
6. S.D. Faust, O.M. Aly. *Adsorption process for water treatment*, Butterworths Publishers, Stoneham, U.K., **1987**.
7. S. Babel, T.A. Kurniawan. *J. Hazard. Mater.* **2003**, B97, 219.
8. A. Bhatnagar, M. Sillanpaa. *Chem. Eng. J.* **2010**, 157, 277.
9. S. de Gisi, G. Lofrano, M. Grassi, M. Notarnicola. *Sustainable Mater. & Technol.* **2016**, 9, 10.
10. R.S. Juang, F.C. Wu, R.L. Tseng. *Colloids & Surf. Physicochem. & Eng. Aspects* **2002**, 201, 191.
11. A. Aygun, S. Yenisoy-Karakas, I. Duman. *Microporous & Mesoporous Mater*. **2003**, 66, 189.
12. R. Malik, D.S. Ramteke, S.R. Wate. *Waste Manag*. **2007**, 27, 1129.
13. Ö. Gerçel, H.F. Gerçel, A.S. Koparal, Ü.B. Ögütveren. *J. Hazard. Mater*. **2008**, 160, 668.
14. L. Ding, B. Zou, W. Gao, Q. Liu, Z. Wang, Y. Guo, X. Wang, Y. Liu. *Colloids & Surf. Physicochem. & Eng. Aspects* **2014**, 446, 1.
15. E.O. Oyelude, F. Frimpong, D. Dawson. *J. Mater. Environ. Sci.* **2015**, 6(4), 1126.
16. W.O. Kumi, J. Takrama, M. Asamoah, E. Gyedu-Akoto, C.K. Agyente-Badu, F.M. Amoah. *A Manual for Extraction of Cocoa Potash and Production of Soft Soap*, Technical Bulletin No. 24, Cocoa Research Institute of Ghana: New Tafo – Akim, Ghana, **2012**.

17. K.Z. Elwakeel, A.M. Elgarahy, S.H. Mohammad. *J. Environ. Chem. Eng*. **2017**, 5, 578.
18. R.P.S. Jeyakumar, V. Chandrasekaran *Asian J. Chem*. **2014**, 26(9), 2545.
19. C. Pongener, D. Kibami, K.S. Rao, R.L. Goswamee, D. Sinha. *Chem. Sci. Trans.* **2015**, 4(1), 59.
20. E.O. Oyelude, J.A.M. Awudza, S.K. Twumasi. *Sci. Reports* **2017**, 7: 12198, DOI: 10.1038/s41598-017-12424-1.
21. G.W. Sears, Jr. *Anal Chem.* **1956**, 28, 1981.
22. R.R. Bansode, J.N. Losso, W.E. Marshall, R.M. Rao, R.J. Portier Bioresour. Technol. **2003**, 90, 175.
23. N. Thinakaran, P. Panneerselvam, P. Baskaralingam, D. Elango, S. Sivanesan *J. Hazard. Mater.* **2008**, 158, 142.
24. A.A. Jafar, S. Balasubramanian *Der Chemica Sinica*. **2010**, 1(2), 35.
25. A.B. Karim, B. Mounir, M. Hachkar, M. Bakasse, Z. Rais, A. Yaacoubi *J. Water Sci. Environ. Technol.* **2017**, 2(2), 200.
26. M. Ghaedi, A. Hassanzadeh, S.N. Kokhdan *J. Chem. Eng. Data* **2011**, 56, 2511.
27. X-Y. Huang, J-P. Bin, H-T. Bu, G-B. Jiang, M-H. Zeng *Carbohydrate Polymers* **2011**, 84, 1350.
28. E.O. Oyelude, F. Appiah-Takyi *Turkish J. Eng. Env. Sci*. **2012**, 36, 161.
29. B.H. Hameed, R.R. Krishni, S.A. Sata *J. Hazard. Mater*. **2009**, 162, 305.
30. M.C. Ncibi, B. Mahjoub, M. Seffen *J. Hazard. Mater*. **2007**, 139, 280.
31. B. Bestani, N. Benderdouche, B. Benstaali, M. Belhakem, A. Addou *Bioresource Technol*. **2008**, 99, 8441.
32. H.I. Chieng, T. Zehra, L.B.L. Lim, N. Priyantha, D.T.B. Tennakoon Environ Earth Sci. **2014**, DOI: 10.1007/s12665-014-3135-7.
33. K.V. Kumar *J. Hazard Mater*. **2006**, 136, 197.
34. L. Langmuir *J. Am. Chem. Soc.* **1918**, 40, 1361.
35. H.M.F. Freundlich *J. Phys. Chem*. **1906**, 57, 385.
36. M.M. Dubinin, L.V. Radushkevich *Proceed. Acad. Sci., Phys. Chem. Section, USSR* **1947**, 55, 331.
37. K.Y. Foo, B.H. Hameed *Chem. Eng. J*. **2010**, 156, 2.
38. S.H. Chien, W.R. Clayton Soil Sci. Soc. Am. J. **1980**, 44, 265.
39. O.S. Bello, M.A. Ahmad, N. Ahmad *Chem & Ecol*. **2012**, 28 (2), 153.
40. K. Fytianosa, E. Voudriasb, E. Kokkalis *Chemosphere* **2000**, 40, 3
41. M.A. Islam, S. Sabar, A. Benhouria, W.A. Khanday, M. Asif, B.H. Hameed J. Taiwan Inst. Chem. Eng. 2017, http://dx.doi.org/10.1016/j.jitce.2017.01.016.
42. S. Lagergren *Kungliga SvenskaVetenskapsakademiens Handlingar* **1898**, 24, 1.
43. Y.S. Ho, G. McKay *Process Biochem*. **1999**, 34, 451.
44. W.J. Weber, J.C. Morris *J. Sanitary Eng. Div., Am. Soc. Civ. Eng*. **1963**, 89, 53.
45. G.E. Boyd, A.W. Adamson, L.S. Meyers Jr. *J. Am. Chem*. Soc. **1947**, 69(11), 2836.
46. U.J. Etim, S.A. Umoren, U.M. Eduok *J. Saudi Chem. Soc*. **2016**, 20, S67.
47. S.S. Gupta, K.G. Bhattacharyya *Adv. Colloids Interface Sci.* **2011**, 162, 39.